Colloids and Surfaces A: Physicochem. Eng. Aspects 419 (2013) 147–155

Contents lists available at SciVerse ScienceDirect

Colloids and Surfaces A: Physicochemical and Engineering Aspects

journal homepage: www.elsevier.com/locate/colsurfa

Synthesis of iron oxide nanoparticles and their application in *Phanerochaete chrysosporium* immobilization for Pb(II) removal

Piao Xu[a,b], Guangming Zeng[a,b,*], Danlian Huang[a,b,*], Shuang Hu[a,b], Chongling Feng[a,b], Cui Lai[a,b], Meihua Zhao[a,b], Chao Huang[a,b], Ningjie Li[a,b], Zhen Wei[a,b], Gengxin Xie[a,b]

[a] College of Environmental Science and Engineering, Hunan University, Changsha 410082, PR China
[b] Key Laboratory of Environmental Biology and Pollution Control (Hunan University), Ministry of Education, Changsha 410082, PR China

HIGHLIGHTS

- A novel biosorbent: MNPs–Ca–alginate immobilized *Phanerochaete chrysosporium* was prepared.
- Optimum biosorption conditions were studied as functions of pH, contact time, etc.
- Optimum conditions were further evaluated by Pearson correlation analysis.
- The biosorbents showed admirable capacity and stability for Pb(II) removal.

GRAPHICAL ABSTRACT

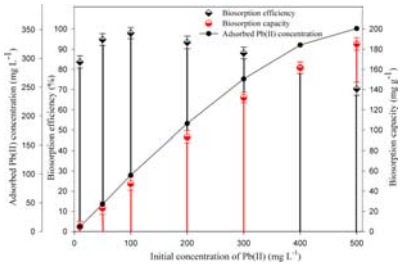

ARTICLE INFO

Article history:
Received 4 June 2012
Received in revised form 23 October 2012
Accepted 30 October 2012
Available online 9 November 2012

Keywords:
Biosorption
Pb(II)
Iron oxide magnetic nanoparticles
Biomass immobilization
Phanerochaete chrysosporium

ABSTRACT

A novel biosorbent was successfully prepared by the immobilization of *Phanerochaete chrysosporium* with iron oxide magnetic nanoparticles (MNPs) and Ca–alginate, which was confirmed by ESEM, EDS, FTIR and XRD characterization. Optimum biosorption conditions were determined as a function of pH, contact time and initial concentration of Pb(II). The maximum biosorption efficiency of Pb(II) was obtained at pH 5.0 and 35 °C, at the value of 96.03%. The uptake of metal was very fast initially, and achieved equilibrium after 8 h. The maximum biosorption capacity reached up to 185.25 mg g^{-1} dry biosorbent at a 500 mg L^{-1} Pb(II)-containing sample. It was obvious that the prepared MNPs–Ca–alginate immobilized *P. chrysosporium* was capable of removing Pb(II) ions from solution efficiently, in terms of its performance and cost. According to Pearson correlation analysis, biosorption efficiency was mostly controlled by contact time and pH, but initial Pb(II) concentration also have a great effect on biosorption efficiency. While the temperature and biosorbent dosage affected at a lower extent. As a result, this work could provide a potential and unique technique for heavy metals removal by enhanced removal capacity and application stability.

1. Introduction

Environmental pollution tends to be one of the most serious problems, which possesses human health risks and causes harmful effect to humanity and other life forms. Especially, heavy metals have been identified as serious environmental contaminants of worldwide concern with a new ranking release recently [1–3]. Heavy metals releasing to the environment causes serious environmental and health risks, because of their toxicities in relatively low concentration, nonbiodegradable and tendency for

* Corresponding authors at: College of Environmental Science and Engineering, Hunan University, Changsha 410082, PR China. Tel.: +86 731 88822754; fax: +86 731 88823701.
E-mail addresses: zgming@hnu.edu.cn (G. Zeng), huangdanlian@hnu.edu.cn (D. Huang).

0927-7757/$ – see front matter © 2012 Elsevier B.V. All rights reserved.
http://dx.doi.org/10.1016/j.colsurfa.2012.10.061

bioaccumulation [4–7]. Many physic-chemical methods like chemical precipitation, ion exchange, reverse osmosis, ultrafiltration, electrochemical treatment, membrane separation, etc. are available for the treatment of heavy metals [8–10]. However, such traditional treatment methods used to heavy metals removal have certain disadvantages such as incomplete metal removal, high cost, energy requirements and generation of secondary pollution [11], and so on.

Recently, biosorption method has been suggested as an efficient, cost-effective and eco-friendly alternative to existing treatment techniques. It tends to be an emerging field of interest, from a both resource conservation and environmental remediation standpoint [12–14]. Research interest into the potential of *Phanerochaete chrysosporium* (*P. chrysosporium*) for biosorption of heavy metals has been widely reported, taking advantage of favorable heavy metal affinity [15,16]. But it is worth noting that the biosorption capacity of *P. chrysosporium* is limited [17,18]. Technologically, immobilization technology is recognized as an effective method to overcome the operational problems of free suspended cells, by providing ideal size, mechanical strength and porous characteristics [19]. First of all, immobilization will assist native microbes in improving their biosorption capacity [20]. Furthermore, the use of immobilization technology also precludes the need to apply in industrial application, because of easy solid–liquid separation, stronger resistance to environmental perturbations and convenience for regeneration [21–23]. Nowadays, a number of studies focus on the use of various polymeric agents as a immobilization carrier, but relatively little work have been done concerning magnetic nanoparticles (MNPs) for the biomass immobilization so far [4,24].

The purpose of this work was to offer an effective biosorbent for Pb(II) removal, subsequently endowing the biosorbent with both great biosorption capacity and practical applicability. Therefore, one such proposed technology combining the adsorption ability of *P. chrysosporium* and MNPs was proposed for the first time proceeded. Besides, various factors, such as pH, contact time and initial concentration of Pb(II), which affected the uptake behavior, were investigated for the determination of optimum biosorption condition. Moreover, Pearson correlation analysis was conducted to examine the relationships between biosorption process and the above factors. The information obtained from these studies was expected to indicate whether the prepared biosorbents had the potential for Pb(II) removal from aqueous solutions.

2. Materials and methods

2.1. Materials

The white-rot basidiomycete, *P. chrysosporium* (BKMF-1767) was maintained by subculturing on potato dextrose agar slants at 4 °C after 7 days cultivation. Spore suspensions were prepared by diluting the spores in sterile distilled water and then adjusted to a concentration of 2.0×10^6 CFU mL^{-1}. All reagents used in the experiment were of analytical reagent grade and used without further purification. Distilled water was used for the preparation of all the solutions throughout this study.

2.2. Preparation of immobilized biosorbents

2.2.1. Synthesize of iron oxide nanoparticles

Iron oxide magnetic nanoparticles were prepared by coprecipitating Fe(II) and Fe(III) in ammonia solution [25]. Firstly, $FeCl_3 \cdot 6H_2O$ (8.5 g) and $FeCl_2 \cdot 4H_2O$ (3.0 g) were dissolved in 38 mL HCl (0.4 M) solution. Chemical precipitation was achieved under vigorous stirring for 30 min by adding 375 mL NH_4OH solution (0.7 M). It was noted that distilled water for both HCl and NH_4OH preparation was previously flushed with N_2 for 10 min. After completely precipitation and stratification, the final nanoparticles were washed three times with distilled water to eliminate free electrolyte. At last, the resultant products were collected by centrifuging at 4000 rpm for 5 min, and then freeze-dried for 24 h for further use.

2.2.2. Immobilization of P. chrysosporium for biosorbents preparation

The immobilization of *P. chrysosporium* was conducted with Ca–alginate and MNPs, by following steps: first, mixed up Na–alginate (40 g L^{-1}, 1 mL) and MNPs (0.10 g), and then sterilization under 115 °C for 30 min; next, the mycelium suspensions (2.0×10^6 CFU mL^{-1}, 0.5 mL) were inoculated into the above mixture, and introduced into sterile $CaCl_2$ (0.1 M, 20 mL) solution for 4 h. As a result, the *P. chrysosporium* – containing MNPs–Ca–alginate microspheres were prepared at the size of about 3–4 mm. After that, the microspheres were rinsed twice with sterile distilled water and then introduced into 250 mL Erlenmeyer flasks containing 50 mL growth medium. Finally, the mixture was incubated at 37 °C and the rotation speed was fixed at 150 rpm. All the above operations were performed under sterile condition. Meanwhile, flasks with free and Ca–alginate immobilized *P. chrysosporium* were used as control samples. After 4–5 days of incubation, all samples were harvested for characterization and biosorption studies. 150 mg of prepared biosorbents were freeze-dried for 24 h at vacuum condition, and then the dry biosorbents were weighted. As a result, wet-to-dry ratio of biosorbents was 300 mg/10 mg.

2.3. Biosorbents characterization

The surface morphological image and elemental composition were obtained from environmental scanning electron microscope (ESEM, FEI QUANTA 200) and energy disperse spectroscopy (EDS, EDAX genesis xm-2) after gold plating at an accelerating voltage of 20 kV. The corresponding Fourier transform infrared spectrophotometer (FTIR) spectra of the biosorbent were recorded on a Nicolet, Nexus-670 FTIR spectrometer over the range 4000–400 cm^{-1}. X-ray powder diffraction (XRD, Rigaku Rotaflex D/Max-C) was used to analyze the composition crystalline structures of biosorbents and performed by a monochromatized X-ray beam with nickel–filtered CuKα radiation (λ = 0.1542 nm).

2.4. Batch biosorption procedures

The freeze-dried biosorbents were used in the biosorption experiments. The factors that affected the biosorption rate and uptake capacity of the biosorbent were examined in a batch system. Batch biosorption tests were conducted by mixing known weight of biosorbents and 50 ml of solution of Pb(II)-containing solution on a shaker at 150 rpm. After biosorption, the residual concentration of Pb(II) in the solution was measured by an atomic absorption spectrometer (AAS, Agilent 3510, USA).

2.5. Statistical analysis

All the experiments were carried out in triplicate and data presented were the mean values from these independent experiments. Standard deviation and error bars were indicated wherever necessary. Statistical analyses were performed using the software package SPSS 18.0 for Windows (SPSS, Germany). The Pearson correlation analyses used to determine the relationships between biosorption efficiency and the tested condition factors, in order to determine the optimum biosorption condition.

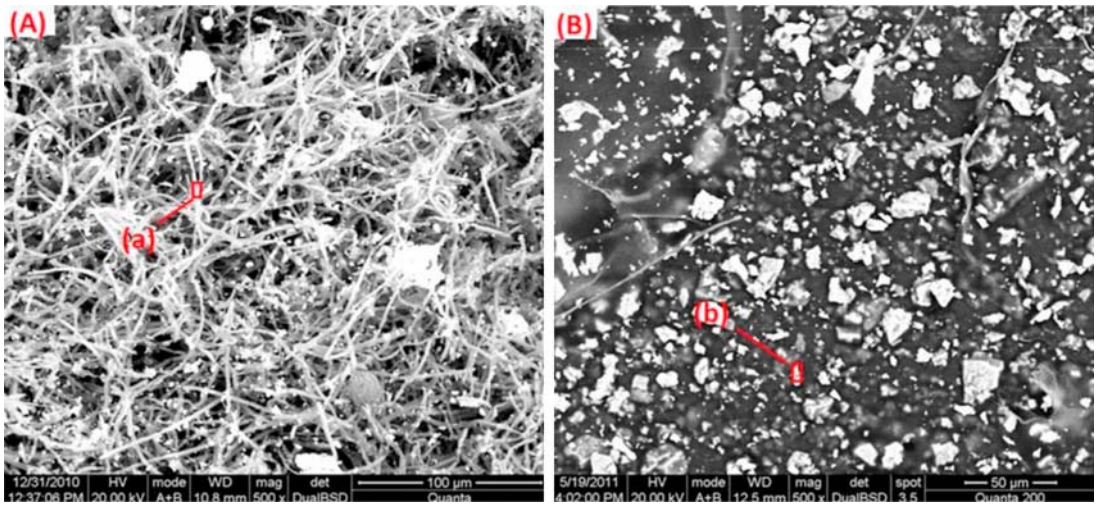

Fig. 1. ESEM images of the surface structure (A) and internal structure (B) of the biosorbents.

3. Results and discussions

3.1. Characterization of biosorbents

3.1.1. Morphology analysis by ESEM

In order to get more direct information about morphology of prepared biosorbents, ESEM micrographs of free and MNPs–Ca–alginate immobilized *P. chrysosporium* were obtained, including surface fungal mycelia along with embedded materials, as shown in Fig. 1. Fig. 1(A) showed the *P. chrysosporium* hyphae micrograph covered at the surface of biosorbents, it was found that the hyphae of immobilized *P. chrysosporium* were packed loosely. The intracellular of the biosorbents had lots of tiny interspaces, offering more adsorptive sites for heavy metals [26]. Thus *P. chrysosporium* could be used as biosorbents for heavy metals. The inside structure of the biosorbents was shown in Fig. 1(B). The micrograph revealed that MNPs were in infinitesimal size and well dispersed in the inside of *P. chrysosporium* hyphae pellet. Additionally, it could be further confirmed by EDS analysis, as shown in Fig. 2. As demonstrated in Fig. 2(a), in *P. chrysosporium* hyphae, elements of C and O accounted for a large proportion (51% and 21%, respectively). From Fig. 2(b), it was found that, Fe possessed a proportion of 17.24% in the inside of the immobilized biosorbents, almost all introduced by Fe_3O_4 nanoparticles. All these results confirmed that MNPs–Ca–alginate immobilized *P. chrysosporium* was successfully prepared.

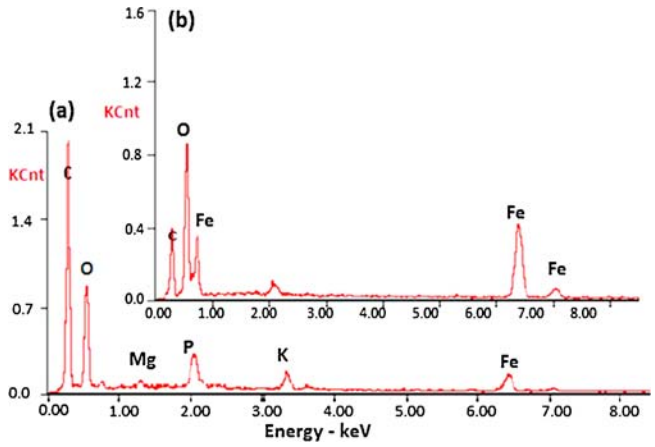

Fig. 2. EDS spectrum of MNPs–Ca–alginate immobilized *P. chrysosporium*. (a) *P. chrysosporium* hyphae at the surface of the biosorbents and (b) iron oxide nanomaterials embedded inside of the MNPs–Ca–alginate immobilized *P. chrysosporium*.

3.1.2. Functional group analysis by FTIR

Fig. 3 depicts the FTIR spectra of the iron oxide magnetic nanoparticles (MNPs), free *P. chrysosporium* and MNPs–Ca–alginate immobilized *P. chrysosporium*. The presence of MNPs could be demonstrated by vibrations of Fe—O bonds of iron oxide by two strong absorption bands at around 628 and 590 cm^{-1} (Fig. 3(a)) [27]. Compared with Fig. 3(b) and (c), peaks assigned to C=O shifted after immobilization, from 1653 cm^{-1} to 1645 cm^{-1}, 1414 cm^{-1} to 1417 cm^{-1}, which indicated that carbonyl groups played an important role in immobilization. The peak 1078 cm^{-1} relating to the stretching vibration of P—OH shifted to 1076 cm^{-1}, while the characteristic absorption band around 1140 cm^{-1} attributed to the vibration of P—O was not observed [27]. The results further reflected the joining of the phosphate groups in the immobilization process. Additionally, the obvious shift took place in the positions of O—H and N—H bending vibration, i.e., from 3359 cm^{-1} to 3394 cm^{-1}, 1041 cm^{-1} to 1039 cm^{-1} [28,29]. These findings implied that the immobilizing process was accomplished via the reaction of a series of functional groups, including O—H, C—OH, C=O, N—H, P—O, P—OH. Especially, the apparent change in the range of 1000–1300 cm^{-1}, which belonged to C—OH stretching and O—H bending [30], suggested that C—OH and O—H played a major role in biomass immobilization. Most importantly, it was obviously found that the bands at around 627 and 586 cm^{-1} appeared, corresponding to the stretching vibrations of Fe—O bonds. It suggested that *P. chrysosporium* was successfully immobilized by MNPs and Ca–alginate.

3.1.3. Structure analysis by XRD

As shown in Fig. 4(a), seven characteristic peaks of Fe_3O_4 (2θ = 31.4, 35.4, 45.7, 55.2, 59.5, 62.5 and 77.5) marked are observed. All the diffraction peaks matched well with result reported by Hu et al. [31]. Importantly, the peaks were significantly broadened, what corresponding to the nanocrystalline character of nanoparticles [6]. The five peaks of the Fe_3O_4 could be observed in Fig. 4(b) for MNPs–Ca–alginate immobilized *P. chrysosporium*, but the intensity declined in a certain degree. The result confirmed that the biosorbents were successfully prepared and the immobilization process did not significantly result in the phase change of Fe_3O_4.

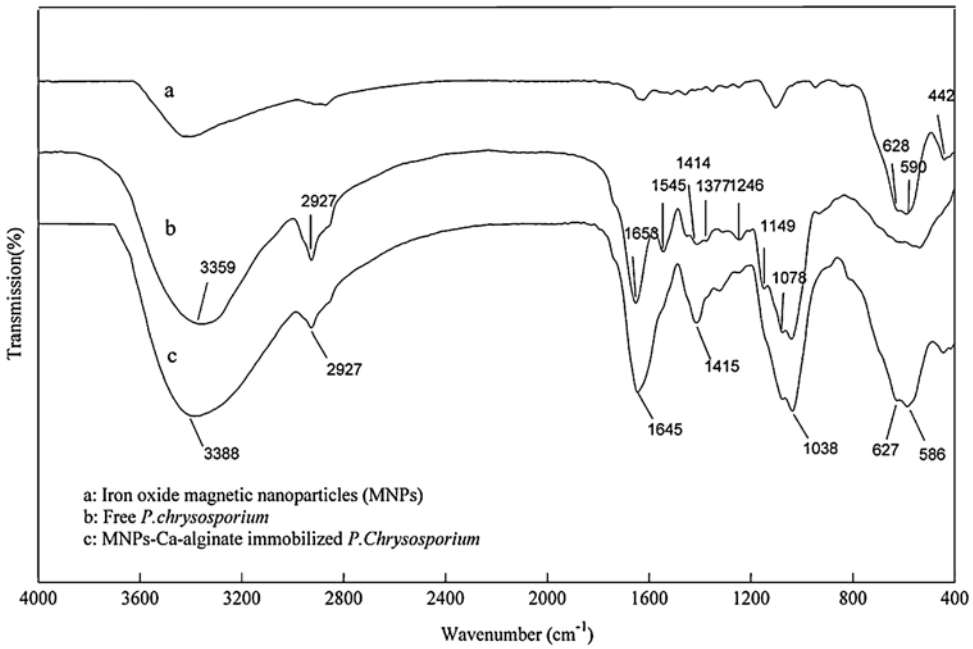

Fig. 3. FTIR spectra for iron oxide magnetic nanoparticles (MNPs) (a), free *P. chrysosporium* (b), and MNPs–Ca–alginate immobilized *P. chrysosporium* (c) in the region between 400 and 4000 cm^{-1}.

3.2. Biosorption experiments

3.2.1. Effect of pH on biosorption

Acidity of metal solutions has been identified as one of the most important controlling parameter in heavy metal biosorption process [13,32]. The binding of H^+ ions to the biomass may be responsible for the variation in biosorption of heavy metals, which compete with metallic ions for active sites on the biosorbent surface [12,33]. In order to establish the effect of pH on Pb(II) biosorption, batch equilibrium studies were conducted at different pH values ranging from 2.0 to 6.5, adjusted by 0.1 M NaOH and HCl. The biosorption experiment was investigated by the free, Ca–alginate and MNPs–Ca–alginate immobilized *P. chrysosporium*, respectively. As a result, metal uptake was affected strongly by variations in pH (Fig. 5).

The variation in biosorption capacity of the selected biosorbents in the detected pH range is shown in Fig. 5. Biosorption capacities of MNPs–Ca–alginate immobilized *P. chrysosporium* were observed at the value of 63.20 and 95.03 mg g^{-1} at pH 2.0 and pH 5.0, respectively. As noticed low biosorption capacity of Pb(II) was found in acidic environment, and an increasing tendency was observed with the increase of pH in the range of 2.0–5.0. The lower uptake of Pb(II) was observed in lower pH value, which might be attributed to large quantities of protons competing with Pb(II) ions for the biosorption site [34]. With the increase of pH, more positively charged Pb(II) ions adsorbed on the free binding sites due to a larger portion of

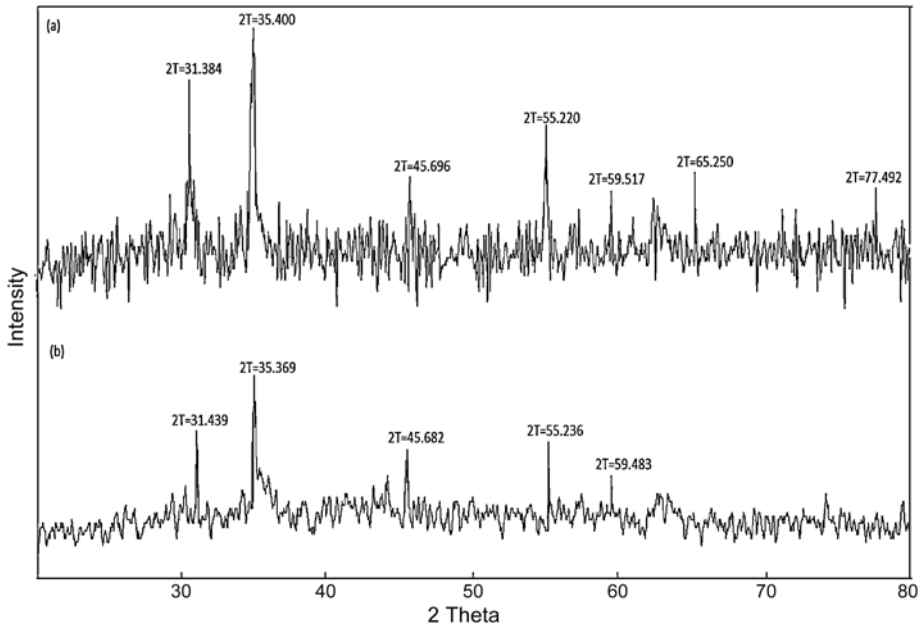

Fig. 4. XRD analysis for Fe_3O_4 MNPs (a), and MNPs–Ca–alginate immobilized *P. chrysosporium* (b).

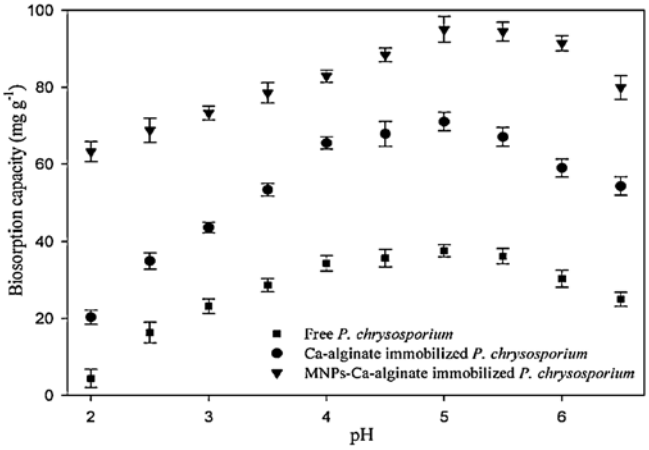

Fig. 5. Effect of pH on the biosorption capacity of the free *P. chrysosporium* (a), Ca–alginate immobilized *P. chrysosporium* (b) and MNPs–Ca–alginate immobilized *P. chrysosporium* (c) for Pb(II) ions. Temperature: 30 °C; initial concentration of Pb(II) ions: 100 mg L^{-1}; biosorbent dosage: 1.0 g L^{-1}. The bars represent the standard deviations of the means ($n = 3$).

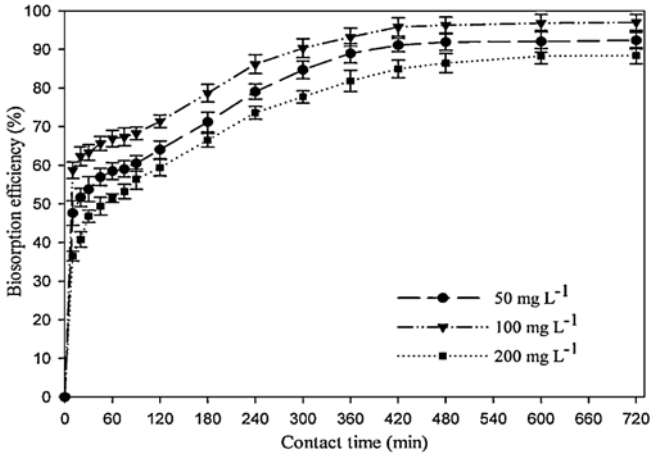

Fig. 6. Effect of contact time on Pb(II) biosorption efficiency. pH value: 5.0; temperature: 35 °C; biosorbent dosage: 1.8 g L^{-1}.

dissociation of protons from functional groups, which resulted in the promotion of biosorption capacity. It was reported that, in the case of biosorption, the interaction not only depended on the nature of the microbes, it might be a consequence of the solution chemistry of the metal ions to be adsorbed [13]. When pH increased to 6, Pb^{2+} and $Pb(OH)^{+}$ were partly translated to $Pb(OH)_2$ [34], which would negatively affect the interactions between chemical groups and Pb(II) ions. Therefore, it was not reasonable to carry out biosorption experiments for Pb(II) at pH > 6.5, which would introduce uncertainty to the results. The maximum biosorption capacity of Pb(II) ions by MNPs–Ca–alginate immobilized *P. chrysosporium* occurred at pH 5.0 at the value of 95.03 mg g^{-1}. According to the results of this initial experiment, further biosorption experiments were performed at pH value of 5.0 as an optimal value.

Additionally, the curves clearly showed that the MNPs–Ca–alginate immobilized *P. chrysosporium* had a higher level of performance for removal of Pb(II) from aqueous medium. The biosorption capacity of Pb(II) increased notably from 37.56 mg g^{-1} (free *P. chrysosporium*) to 95.03 mg g^{-1} by MNPs–Ca–alginate immobilization at pH 5.0. Even by Ca–alginate immobilization, the maximum capacity was 71.04 mg g^{-1}, which was much lower than MNPs–Ca–alginate immobilized *P. chrysosporium* (95.03 mg g^{-1}). It further implied that MNPs played vital roles in the biosorption ability improvement. Importantly, the biosorption capacity of MNPs–Ca–alginate immobilized *P. chrysosporium* exceeded 65 mg g^{-1} even at acid and neutral pH, while the free *P. chrysosporium* showed poor ability (below 40 mg g^{-1}). It further suggested that the prepared biosorbents showed great biosorption ability to Pb(II), even it could be expected that the stability of the prepared biosorbents were greatly augmented.

3.2.2. Effect of contact time

The rate of biosorption was important for designing batch biosorption studies [35]. In this study, time-course profile for the biosorption of 50, 100 and 200 mg L^{-1} Pb-containing solution by Ca–alginate–MNPs immobilized *P. chrysosporium* is presented in Fig. 6. As observed, the biosorption of Pb(II) increased considerably with increasing of contact time at the beginning of biosorption, from 0 to 1 h. It was mainly because that Pb(II) existing in aqueous solution was firstly adsorbed to the biosorbent surface (mainly *P. chrysosporium* hyphae). After that, the biosorption capacity kept a continued increasing tendency, at a slower rate, followed by a longer equilibrium period from 1 h to 8 h. The reason for the continued ascent was probably that Pb(II) ions slowly transmitted to the interior of biosorbents (mainly iron oxide MNPs and Ca–alginate) with the saturation of surface binding sites. After this equilibrium period, further increases in contact time did not enhance the biosorption yield, suggesting that the biosorption reached saturation at 8 h.

Results in our study were in accord with the study by Yetis et al. [36], who demonstrated that biosorption occurred at two stages: the first was the rapid surface binding and the second was the slow intra-diffusion. Especially in the presence of MNPs, intra-diffusion occurred in the interior of biosorbents might be further enhanced, and then the saturation of function groups would be put off consequently extending biosorption process. Additionally, the maximum biosorption efficiency of Pb(II) with initial concentration of 50, 100, 200 mg L^{-1} reached 92.30%, 96.98% and 88.41%, respectively, suggesting that the prepared biosorbents were effective at various initial concentration. Despite the equilibrium time was about 8 h, a 12 h of contact time was adopted for the subsequent experiment to ensure the biosorption equilibrium.

3.2.3. Effect of biosorption temperature

Temperature played key roles in the biosorption process. In this study, biosorption of Pb(II) by free, Ca–alginate immobilized *P. chrysosporium*, MNPs and MNPs–Ca–alginate immobilized *P. chrysosporium* appears to be temperature independent in the temperature range of 20–45 °C (Fig. 7). It was apparent that the biosorption efficiency for Pb(II) gradually elevated with the increase in temperature from 20 °C to 35 °C. It has been suggested that increase in metal uptake at increased temperature was due to either higher affinity of sites for metal or an increase in binding sites on relevant biomass [37]. Additionally, increasing the temperature would decrease the viscosity of the solution which enhanced the rate of diffusion of the adsorbate molecules across the external boundary layer of the biosorbent and resulted in higher biosorption efficiency [38].

At all the temperature tested, the highest removal efficiency was observed at 35 °C with MNPs–Ca–alginate immobilized *P. chrysosporium* at the value of 95.17%. It demonstrated that the biosorption efficiency was enhanced to a great extent by MNPs–Ca–alginate immobilization. Firstly, porosity in Ca–alginate allowed Pb(II) to diffuse into the interior of biosorbents and come in contact with the entrapped mediums, so that removal efficiency of Ca–alginate immobilized *P. chrysosporium* has been heightened (62.86%). Moreover, besides Ca–alginate and *P. chrysosporium*, MNPs also had considerable adsorption ability to Pb(II), the maximal efficiency was 70.4% at 35 °C. The heavy metals adsorbed to

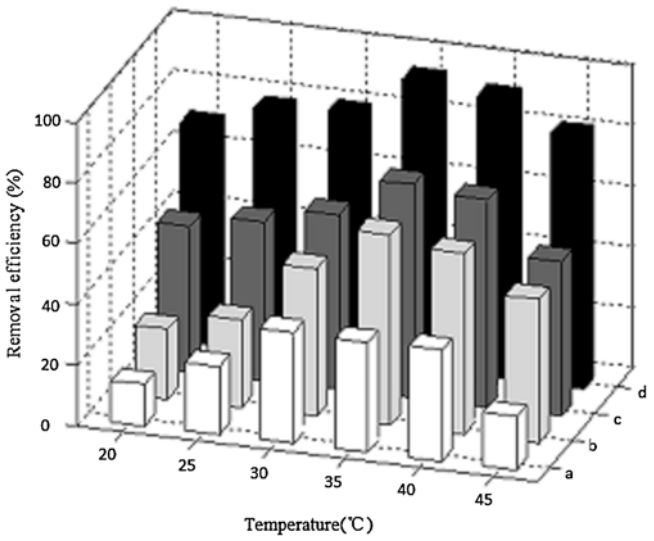

Fig. 7. Effect of temperature on Pb(II) biosorption efficiency by free *P. chrysosporium* (a), Ca–alginate immobilized *P. chrysosporium* (b), iron oxide nanoparticles (c) and MNPs–Ca–alginate immobilized *P. chrysosporium* (d). pH value: 5.0; contact time: 12 h; biosorbent dosage: 1.0 g L^{-1}; Pb(II) concentration: 100 mg L^{-1}.

the surface might transmit to the interior of the biosorbents due to the electrostatic attraction between MNPs and heavy metal ions [39], which resulted in the enhancement of biosorption capacity of biosorbents.

3.2.4. Effect of biosorbent dosage

An optimum biosorbent dosage is essentially required to maximize the interactions between metal ions and biosorption sites of biosorbent [40]. To evaluate the optimum dosage of biosorbent, 0.45–2.7 g of freshly prepared MNPs–Ca–alginate immobilized *P. chrysosporium* biosorbents were added to 50 mL of Pb-containing aqueous solution at the concentration of 100 mg L^{-1}. Evidently, the biosorption percentage and equilibrium capacity were sensitive to the variation of biosorbent content. Fig. 8 illustrated an elevation of the removal percent with the increasing in biosorbent dosage. This result might be attributed to that increasing the dosage of biosorbents would increase the density of reactive groups available for metal binding and on the external surface area of the biosorbent. Additionally, the increasing biosorbent dose may affect the concentration gradient between the surface of the biosorbent and the internal groups due to the change in the concentration of the solution [41]. More biosorption sites were supplied by larger dosage of biosorbents, therefore resulted in higher removal efficiency. While the subdued increasing trend of efficiency emerged at a higher dosage than 1.5 g L^{-1}, which could be explained as a consequence of partial aggregation of biosorbent, consequently contributing to the decrease in effective surface area for the biosorption [12].

On the other hand, if the results were expressed in Pb(II) removal capacity, the values exhibited opposite trend with removal efficiency. It illustrated that the biosorption capacity decreased with an increase in biosorbent dosage. As the biosorbent dosage increased from 0.3 to 1.8 g L^{-1}, the biosorption capacity for Pb(II) decreased from 194.43 mg/g to 51.78 mg/g. The decrease in biosorption capacity might be resulted from interference existed between binding sites and biosorbent, or insufficiency of metal ions in solution with respect to available binding sites [42]. Moreover, overlapping of biosorption sites as a result of overcrowding of biosorbents may also resulted in the decrease of biosorption capacity [43].

Table 1
A comparison of maximal adsorption capacities (q_m) of white-rot fungi biosorbents and magnetic adsorbents used for Pb(II) removal.

Adsorbents	q_m (mg/g)	Cycles	Reference
Fe_3O_4 MNPs	36.0 mg/g	5	[38]
m-PAA-Na-coated MNPs	40.0 mg/g	3	[47]
Magnetic alginate beads	100 mg/g	5	[5]
Free *Phanerochaete chrysosporium*	80 mg/g	–	[36]
Loofa sponge immobilized *P. chrysosporium*	135.3 mg/g	5	[11]
Ca–alginate immobilized *P. chrysosporium*	63.7 mg/g	–	This study
MNPs–Ca–alginate immobilized *P. chrysosporium*	185.25 mg/g	5	This study

3.2.5. Effect of Pb(II) initial concentration

The biosorption capacity was a function of the initial concentration of Pb(II). To measure the biosorption ability, biosorption experiments were carried out with the wide ranges of initial total metal ion concentration of 10–500 mg L^{-1}. The results, in terms of Pb(II) biosorption efficiency and capacity versus initial concentration of Pb(II), are presented in Fig. 9. Normally, the conventional biosorbents were not suitable to remove metal ions in low concentrations (less than 100 ppm). However, it was evident that the prepared biosorbents were quite effective for Pb(II) removal. Even at an extremely low concentration of 10 mg L^{-1}, the biosorption efficiency reached up to 83.68%. Therefore, as-prepared biosorbents showed a promising prospect for application in trace metal removal. Moreover, it could be observed that the removal efficiency enhanced with the increasing of Pb(II) concentration below 100 mg L^{-1}. This increase might be due to a reinforce in electrostatic interactions (relative to covalent interactions) with increasing Pb(II) concentration [44]. In addition, it has been demonstrated that the initial concentration supplied a kind of important driving force to overcome the existing mass transfer resistance of Pb(II) ions between the aqueous and solid phases [45]. The maximum biosorption efficiency was 94.96% at the initial Pb(II) concentration of 100 mg L^{-1}. However, the biosorption efficiency presented a declining trend while the Pb(II) concentration was elevated above 200 mg L^{-1}. It seemed to be a result of insufficient available sites on the surface of biosorbents and saturation in the interior of biosorbents, subsequently resulting in the saturation of biosorption sites and decline of the biosorption efficiency [46].

Additionally, as we expected, the overall trend of biosorption capacity was an increase with increasing of initial Pb(II) concentrations. But the initial slope was much greater affected by the variation of biosorption capacity than in the case of biosorption efficiency. In the case of MNPs–Ca–alginate immobilized *P. chrysosporium*, the maximum biosorption capacity was 185.25 mg g^{-1} dry biosorbent in the presence of 500 mg L^{-1} Pb(II) ions, which was much higher than other reported adsorbents. A comparison of maximum adsorption capacities (q_m) of white-rot fungi biosorbents and magnetic nanosorbents for Pb(II) removal has been given in Table 1. A perusal of Table 1 showed that the novel biosorbent used in the present study was an efficient material for removal of Pb(II) from aqueous solution.

3.3. Statistical analysis

Pearson correlation analysis was conducted to evaluate the relationships between biosorption efficiency and biosorption conditions, such as pH, contact time, temperature, biosorbent dosage and initial Pb(II) concentration (Table 2). As expected, the most significant correlations between biosorption efficiency and contact time were observed, which was consistent with previous results that biosorption efficiency increased with increasing contact time,

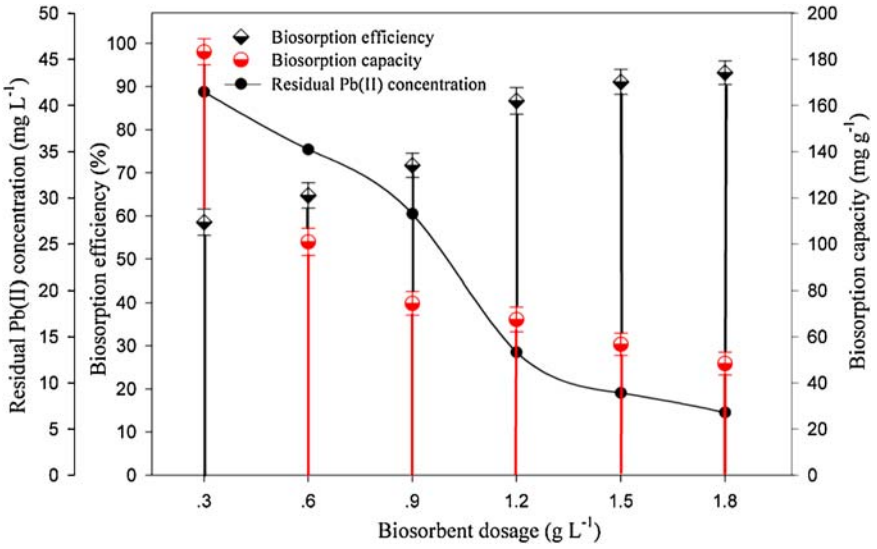

Fig. 8. Effect of biosorbent dosage on Pb(II) biosorption efficiency. pH value: 5.0; temperature: 35 °C, Pb(II) concentration: 100 mg L^{-1}.

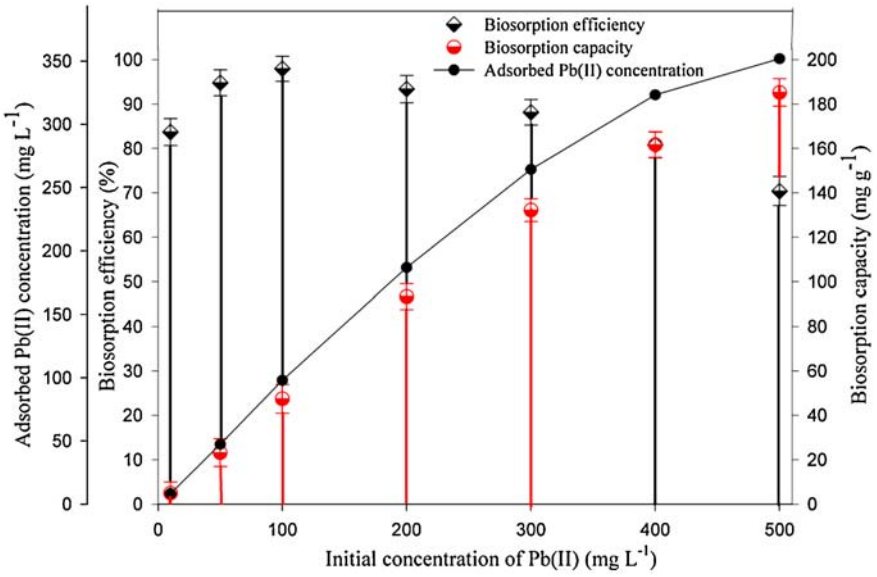

Fig. 9. Effect of initial Pb(II) concentration on biosorption efficiency and capacity. pH value: 5.0; temperature: 35 °C; biosorbent dosage: 2.0 g L^{-1}.

Table 2
Pearson correlation matrix of biosorption efficiency and biosorption conditions observed in experiments.

	Efficiency	pH	Time	Temperature	Dosage	Concentration
Efficiency	1					
pH	0.231*	1				
Contact time	0.480**	−0.338**	1			
Temperature	0.062	−0.048	−0.265*	1		
Dosage	0.132	−0.078	0.098	−0.102	1	
Concentration	−0.427**	0.030**	0.164	−0.303**	−0.063	1

* Correlation is significant at the 0.05 level (two-tailed).
** Correlation is significant at the 0.01 level (two-tailed).

suggesting that adequate contact time for effective removal was quite essential. In addition, biosorption efficiency positively correlated with pH, which suggested that pH affected the biosorption process to a large extent. Meanwhile, no significant correlations were observed for the temperature and biosorbent dosage respectively, therefore the biosorbents showed an enhanced stability to temperature in a large range of dosages. While a negative correlation was obtained between biosorption efficiency and initial concentration, as a result of the definite occupancy number of biosorbents.

4. Conclusions

In this work, MNPs–Ca–alginate immobilized *P. chrysosporium* biosorbents were successfully prepared and characterized by ESEM, EDS, XRD and FTIR. Meanwhile, abundant results demonstrated

that the prepared biosorbents showed a promising prospect for application in heavy metal wastewater treatment. It was found that biosorption efficiency was dependent on experimental conditions. The biosorption efficiency was highly pH dependent and increased with an increase of pH in the range of 2.0–5.0. The optimal biosorption occurred at pH 5.0 and 35 °C. In addition, the biosorption efficiency quickly increased at first 1 h, and then kept a continued increasing tendency at a slower rate, followed by a longer equilibrium period at 8 h. The biosorption capacity for Pb(II) (188.25 mg g^{-1}) was significantly higher than conventional adsorbents. Additionally, by Pearson correlation analysis, it was suggested that the biosorption efficiency was highly time and pH dependent, and affected by initial Pb(II) concentration at a large extent, while the temperature and biosorbent dosage affected at a lower extent. In summary, iron oxide nanoparticles combined with Ca–alginate were available immobilization carries for the entrapment of *P. chrysosporium* to prepare effective biosorbent for Pb(II) removal [38,47].

Acknowledgments

The study was financially supported by the National Natural Science Foundation of China (51039001, 50808073, 50978088), the Hunan Key Scientific Research Project (2009FJ1010), the Hunan Provincial Natural Science Foundation of China (10JJ7005), the Environmental Protection Technology Research Program of Hunan (2007185), the New Century Excellent Talents in University (NCET-08-0181) and the Xiangjiang Water Environmental Pollution Control Projects Subjected to the National Key Science and Technology Project for Water Environmental Pollution Control (2009ZX0 7212-001-02 and 2009ZX0 7212-001-06).

References

[1] Y. Pang, G.M. Zeng, L. Tang, Y. Zhang, Y.Y. Liu, X.X. Lei, Z. Li, J.C. Zhang, Z.F. Liu, Y.Q. Xiong, Preparation and application of stability enhanced magnetic nanoparticles for rapid removal of Cr(VI), Chem. Eng. J. 175 (2011) 222–227.
[2] J.S. Lim, S.M. Kim, S.Y. Lee, E.A. Stach, J.N. Culver, M.T. Harris, Quantitative study of Au(III) and Pd(II) ion biosorption on genetically engineered Tobacco mosaic virus, J. Colloid Interface Sci. 342 (2010) 455–461.
[3] A.B. Cundy, L. Hopkinson, R.L.D. Whitby, Use of iron-based technologies in contaminated land and groundwater remediation: a review, Sci. Total Environ. 400 (2008) 42–51.
[4] P. Xu, G.M. Zeng, D.L. Huang, C.L. Feng, S. Hu, M.H. Zhao, C. Lai, Z. Wei, C. Huang, G.X. Xie, Z.F. Liu, Use of iron oxide nanomaterials in wastewater treatment: a review, Sci. Total Environ. 424 (2012) 1–10.
[5] A. Bée, D. Talbot, S. Abramson, V. Dupuis, Magnetic alginate beads for Pb(II) ions removal from wastewater, J. Colloid Interface Sci. 362 (2011) 486–492.
[6] M. Bystrzejewski, K. Pyrzyńska, A. Huczko, H. Lange, Carbon-encapsulated magnetic nanoparticles as separable and mobile sorbents of heavy metal ions from aqueous solutions, Carbon 47 (2009) 1201–1204.
[7] J. Wang, C. Chen, Biosorbents for heavy metals removal and their future, Biotechnol. Adv. 27 (2009) 195–226.
[8] G.M. Zeng, X. Li, J.H. Huang, C. Zhang, C.F. Zhou, J. Niu, L.J. Shi, S.B. He, F. Li, Micellar-enhanced ultrafiltration of cadmium and methylene blue in synthetic wastewater using SDS, J. Hazard. Mater. 185 (2011) 1304–1310.
[9] H.J. Guo, S.L. Luo, L. Chen, X. Xiao, Q.A. Xi, W.Z. Wei, G.M. Zeng, C.B. Liu, Y. Wan, J.L. Chen, Y.J. He, Bioremediation of heavy metals by growing hyperaccumulaor endophytic bacterium *Bacillus* sp *L14*, Bioresour. Technol. 101 (2010) 8599–8605.
[10] X. Li, G.M. Zeng, J.H. Huang, D.M. Zhang, L.J. Shi, S.B. He, M. Ruan, Simultaneous removal of cadmium ions and phenol with MEUF using SDS and mixed surfactants, Desalination 276 (2011) 136–141.
[11] M. Iqbal, Biosorption of lead, copper and zinc ions on loofa sponge immobilized biomass of *Phanerochaete chrysosporium*, Miner. Eng. 17 (2004) 217–223.
[12] V.K. Gupta, A. Rastogi, A. Nayak, Biosorption of nickel onto treated alga (*Oedogonium hatei*): application of isotherm and kinetic models, J. Colloid Interface Sci. 342 (2010) 533–539.
[13] H. Seki, A. Suzuki, H. Maruyama, Biosorption of chromium(VI) and arsenic(V) onto methylated yeast biomass, J. Colloid Interface Sci. 281 (2005) 261–266.
[14] S.J.T. Pollard, F.E. Thompson, G.L. Mcconnachie, Microporous carbons from moringa oleiferahusks for water purification in less developed countries, Water Res. 29 (1995) 337–347.
[15] M. Iqbal, R. Edyvean, Loofa sponge immobilized fungal biosorbent: a robust system for cadmium and other dissolved metal removal from aqueous solution, Chemosphere 61 (2005) 510–518.
[16] D.L. Huang, G.M. Zeng, X.Y. Jiang, C.L. Feng, H.Y. Yu, G.H. Huang, H.L. Liu, Bioremediation of Pb-contaminated soil by incubating with *Phanerochaete chrysosporium* and straw, J. Hazard. Mater. 134 (2006) 268–276.
[17] C.S. Rodriguez, Dye removal by immobilised fungi, Biotechnol. Adv. 27 (2009) 227–235.
[18] D.L. Huang, G.M. Zeng, X.Y. Jiang, C.L. Feng, S. Hu, M.H. Zhao, C. Lai, Y. Zhang, X.Y. Jiang, H.L. Liu, Mycelial growth and solid-state fermentation of lignocellulosic waste by white-rot fungus *Phanerochaete chrysosporium* under lead stress, Chemosphere 81 (2010) 1091–1097.
[19] G.M. Zeng, D.L. Huang, G.H. Huang, T.J. Hu, X.Y. Jiang, C.L. Feng, Y.N. Chen, L. Tang, H.L. Liu, Composting of lead-contaminated solid waste with inocula of white-rot fungus, Bioresour. Technol. 98 (2007) 320–326.
[20] C.S. Rodriguez, M.A. Sanroman, D. Hofer, G. Gubitz, Stainless steel sponge: a novel carrier for the immobilisation of the white-rot fungus *Trametes hirsuta* for decolourization of textile dyes, Bioresour. Technol. 95 (2004) 67–72.
[21] K. Yasemin, A. Cigdem, T. Sema, D. Adil, G. Omer, A.M. Yakup, Biosorption of Hg(II) and Cd(II) from aqueous solutions, Process Biochem. 37 (2002) 601–610.
[22] M. Shin, T. Nguyen, J. Ramsay, Evaluation of support materials for the surface immobilization and decoloration of amaranth by *Trametes versicolor*, Appl. Microbiol. Biotechnol. 60 (2002) 218–223.
[23] J. Wu, H.Q. Yu, Biosorption of 2,4-dichlorophenol by immobilized white-rot fungus *Phanerochaete chrysosporium* from aqueous solutions, Bioresour. Technol. 98 (2007) 253–259.
[24] Q.Q. Peng, Y.G. Liu, G.M. Zeng, W.H. Xu, C.P. Yang, J.J. Zhang, Biosorption of copper(II) by immobilizing *Saccharomyces cerevisiae* on the surface of chitosan-coated magnetic nanoparticles from aqueous solution, J. Hazard. Mater. 177 (2010) 676–682.
[25] Y. Zhang, G.M. Zeng, L. Tang, H.Y. Yu, J.B. Li, Catechol biosensor based on immobilizing laccase to modified core–shell magnetic nanoparticles supported on carbon paste electrode, Environ. Sci. 28 (2007) 2320–2325.
[26] D.L. Huang, G.M. Zeng, C.L. Feng, S. Hu, X.Y. Jiang, L. Tang, F.F. Su, Y. Zhang, W. Zeng, H.L. Liu, Degradation of lead-contaminated lignocellulosic waste by *Phanerochaete chrysosporium* and the reduction of lead toxicity, Environ. Sci. Technol. 42 (2008) 4946–4951.
[27] M. Ma, Y. Zhang, W. Yu, H.Y. Shen, H.Q. Zhang, N. Gu, Preparation and characterization of magnetite nanoparticles coated by amino silane, Colloids Surf. A 212 (2003) 219–226.
[28] G. Bayramoğlu, G. Çelik, M.Y. Arica, Biosorption of heavy metal ions on immobilized white-rot fungus *Trametes versicolor*, J. Hazard. Mater. 101 (2003) 285–300.
[29] N.S. Kumar, K. Min, Phenolic compounds biosorption onto *Schizophyllum commune* fungus: FTIR analysis, kinetics and adsorption isotherms modeling, Chem. Eng. J. 168 (2011) 562–571.
[30] S.X. Zhang, H.Y. Niu, Z.J. Hu, Y.Q. Cai, Y.L. Shi, Preparation of carbon coated Fe_3O_4 nanoparticles and their application for solid-phase extraction of polycyclic aromatic hydrocarbons from environmental water samples, J. Chromatogr. A 1217 (2010) 4757–4764.
[31] H.B. Hu, Z.H. Wang, L. Pan, Synthesis of monodisperse Fe_3O_4–silica core–shell microspheres and their application for removal of heavy metal ions from water, J. Alloys Compd. 492 (2010) 656–661.
[32] R. Say, A. Denizli, M.Y. Arica, Biosorption of cadmium(II), lead(II) and copper(II) with the flamentous fungus *Phanerochaete chrysosporium*, Bioresour. Technol. 76 (2001) 67–70.
[33] P. Lodeiro, J.L. Barriada, R. Herrero, M.E. Sastre de Vicente, The marine macroalga *Cystoseira baccata* as biosorbent for cadmium(II) and lead(II) removal: kinetic and equilibrium studies, Environ. Pollut. 142 (2006) 264–273.
[34] T.K. Naiya, A.K. Bhattacharya, S.K. Das, Adsorption of Pb (II) by sawdust and neem bark from aqueous solutions, Environ. Prog. 27 (2008) 313–328.
[35] Y. Gutha, V.S. Munagapati, S.R. Alla, K. Abburi, Biosorptive removal of Ni (II) from aqueous solution by *Caesalpinia bonducella* seed powder, Sep. Sci. Technol. 46 (2011) 2291–2297.
[36] U. Yetis, A. Dolek, F.B. Dilek, G. Ozcengiz, The removal of Pb(II) by *Phanerochaete chrysosporium*, Water Res. 34 (2000) 4090–4100.
[37] A.M. Marques, X. Roca, M.D. Simon-Pujol, M.C. Fuste, F. Congregado, Uranium accumulation by *Pseudomonas* sp. EPS-5028, Appl. Microbiol. Biotechnol. 35 (1991) 406–410.
[38] N.N. Nassar, Rapid removal and recovery of Pb(II) from wastewater by magnetic nanoadsorbents, J. Hazard. Mater. 184 (2010) 538–546.
[39] L.S. Zhong, J.S. Hu, H.P. Liang, A.M. Cao, W.G. Song, L.J. Wan, Self-assembled 3D flowerlike iron oxide nanostructures and their application in water treatment, Adv. Mater. 18 (2006) 2426–2431.
[40] Y.T. Zhou, H.L. Nie, C. Branford-White, Z.Y. He, L.M. Zhu, Removal of Cu^{2+} from aqueous solution by chitosan-coated magnetic nanoparticles modified with α-ketoglutaric acid, J. Colloid Interface Sci. 330 (2009) 29–37.
[41] C. Boschi, H. Maldonado, M. Ly, E. Guibal, Cd(II) biosorption using *Lessonia kelps*, J. Colloid Interface Sci. 357 (2011) 487–496.
[42] T. Fan, Y.G. Liu, B.Y. Feng, G.M. Zeng, C.P. Yang, M. Zhou, H.Z. Zhou, Z.F. Tan, X. Wang, Biosorption of cadmium(II), zinc(II) and lead(II) by *Penicillium simplicissimum*: isotherms, kinetics and thermodynamics, J. Hazard. Mater. 160 (2008) 655–661.
[43] H. Lata, V. Garg, R. Gupta, Adsorptive removal of basic dye by chemically activated *Parthenium* biomass: equilibrium and kinetic modeling, Desalination 219 (2008) 250–261.

[44] S. Paul, D. Bera, P. Chattopadhyay, L. Ray, Biosorption of Pb(II) by *Bacilus cereus* M16 immobilized in calcium alginate gel, J. Hazard. Subst. Res. 5 (2006) 1–13.
[45] M. Iram, C. Guo, Y.P. Guan, A. Ishfaq, H.Z. Liu, Adsorption and magnetic removal of neutral red dye from aqueous solution using Fe_3O_4 hollow nanospheres, J. Hazard. Mater. 181 (2010) 1039–1050.
[46] M. Erdem, F. Gur, F. Tumen, Cr(VI) reduction in aqueous solutions by siderite, J. Hazard. Mater. 113 (2004) 217–222.
[47] A.R. Mahdavian, M.A.S. Mirrahimi, Efficient separation of heavy metal cations by anchoring polyacrylic acid on superparamagnetic magnetite nanoparticles through surface modification, Chem. Eng. J. 159 (2010) 264–271.